

Article

Evaluation of Surface Characteristics and Hemocompatibility on the Oxygen Plasma-Modified Biomedical Titanium

Hsi-Jen Chiang ^{1,2}, Hsin-Hua Chou ^{2,3}, Keng-Liang Ou ^{4,5,6,7,8,9} , Erwan Sugiarno ⁸, Muhammad Ruslin ¹⁰, Rahmat Abd Waris ^{2,6}, Chiung-Fang Huang ^{4,11}, Chung-Ming Liu ^{12,13,*} and Pei-Wen Peng ^{11,*}

¹ Graduate Institute of Biomedical Materials and Tissue Engineering, College of Biomedical Engineering, Taipei Medical University, Taipei 110, Taiwan; chj621008@gmail.com

² School of Dentistry, College of Oral Medicine, Taipei Medical University, Taipei 110, Taiwan; hhchou@tmu.edu.tw (H.-H.C.); rahmatwariz@yahoo.co.id (R.A.W.)

³ Dental Department of Wan-Fang Hospital, Taipei Medical University, Taipei 116, Taiwan

⁴ Department of Dentistry, Taipei Medical University Hospital, Taipei 110, Taiwan; klou@tmu.edu.tw (K.-L.O.); d642078@yahoo.com.tw (C.-F.H.)

⁵ Department of Dentistry, Taipei Medical University-Shuang Ho Hospital, New Taipei City 235, Taiwan

⁶ Department of Prosthodontic, Faculty of Dentistry, Hasanuddin University, Makassar 90245, Indonesia

⁷ School of Dentistry, Health Sciences University of Hokkaido, Hokkaido 061-0293, Japan

⁸ Department of Prosthodontic, Faculty of Dentistry, Universitas Gadjah Mada, Yogyakarta 55281, Indonesia; erwansugiarno@ugm.ac.id

⁹ 3D Global Biotech Inc., New Taipei City 221, Taiwan

¹⁰ Department of Oral and Maxillofacial Surgery, Faculty of Dentistry, Hasanuddin University, Makassar 90245, Indonesia; ruslin_oms@yahoo.com

¹¹ School of Dental Technology, Taipei Medical University, Taipei 110, Taiwan

¹² School of Dentistry, College of Medicine, China Medical University, Taichung 404, Taiwan

¹³ Biomedical Technology R & D Center, China Medical University Hospital, Taichung 404, Taiwan

* Correspondence: liuc@mail.cmu.edu.tw (C.-M.L.); apon@tmu.edu.tw (P.-W.P.);

Tel.: +886-4-22073105 (C.-M.L.); +886-2-27372181 (ext. 5130) (P.-W.P.)

Received: 14 May 2018; Accepted: 30 June 2018; Published: 3 July 2018



Abstract: Oxygen plasma with different treatment powers and durations was utilized to modify the biomedical pure titanium (Ti) surface in the present study. The superficial, microstructural and biological properties of the plasma-oxidized samples were investigated using the electron microscopy, X-ray photoemission spectroscopy, grazing incidence X-ray diffractometer, contact angle goniometer and blood clotting time assay. During different treatment powers and durations, the island-like nanostructural rutile-TiO₂ layer and dimple-like nanostructural rutile-TiO₂ layer were generated on the surfaces of the plasma-oxidized samples, respectively. It was also found that the plasma-oxidized sample with a rough oxide layer resulted in the formation of a higher wettability. Moreover, the blood clotting time assay indicated that the plasma-oxidized samples exhibited the adhesion behaviors of red blood cells. As the Ti surface underwent plasma oxidation at 280 W for 30 min, it not only generates a rough nanostructural rutile-TiO₂ layer, but also presents an excellent hemocompatibility. Therefore, these findings demonstrate that oxygen plasma modification is a potential approach to promote the hemocompatibility of biomedical pure Ti surface.

Keywords: oxygen plasma treatment; titanium dioxide; wettability; hemocompatibility

1. Introduction

Some biological moieties have been adopted in conjunction with artificial implants such as platelet-derived growth factors and insulin-like growth factors, which have been used at the insertion site of titanium (Ti) dental implants in animals [1,2]. These kinds of dental implants have several effects on promoting bone tissue regeneration. Similarly, bone morphogenetic proteins have an osteoinductive effect when they were coated onto dental implants or coupled with other carriers [3–6]. However, these adsorption techniques of bioactive products at the implantation site have certain drawbacks, including the potential for undesirable release and diffusion of biological molecules far from the interface between the material and tissue, as well as a necessity for relatively large quantities of protein. The implant surface can change with time, no matter what material it is. Particular attention must be given to the stability of the material surface.

It is well known that the biomaterial implanted into the human body caused subsequent damage to the surrounding tissues and increased susceptibility to infection [7]. A common cause of persistent inflammatory processes and the ultimate failure of implants is the adherence of microorganisms to the surface and the formation of complex biofilms at the interface between the biomaterial and the biological environment [8–10]. The inflammatory response and routine sterilization itself can modify the biomaterial surface characteristic [11,12]. Moreover, the surface characteristics of Ti implants, such as topography, microstructure and wettability, also play vital roles in enhancing in vivo osseointegration, since the topography and microstructure characteristics induce surface wettability variation. Thus, the implants need careful and controllable modification of their surface properties [10,13,14].

Ti oxides are recognized as a promising biomaterial with proven biocompatibility [15,16]. Plasma oxidation treatment is a potential green processing technology to generate the oxide layers, because it possesses some advantages such as an all-dry process (decreasing water consumption), environmental friendliness (no waste chemicals), ability to treat temperature sensitive materials and low unit cost per treatment in comparison with other common anodic and thermal oxidation methods [17]. Moreover, Göttlicher et al. [18] also reported the possible mechanisms for plasma oxidation (low energy ion bombardment by negative oxygen ions) on the formation of nanocrystalline stoichiometric TiO₂ oxide layers. Accordingly, the plasma-modified Ti oxide layers have been widely investigated as coatings for enhancing osteogenic activity and in vivo osseointegration of the Ti dental implants. Previous studies have demonstrated that the formation of rutile TiO₂ can enhance its hemocompatibility (relating to blood platelets and blood clotting cascade) [19–21]. Blood clotting or thrombus formation proceeds through two pathways: one is the route in which several proteins or factors are activated in a cascade manner, and the other is associated with platelet activation [22]. From a clinical application of view, it would be desirable if the traditional Ti dental implant surface could be modified as the high biocompatibility and hemocompatibility Ti oxide surface without sacrificing desirable physicochemical and biological properties. Therefore, the purpose of the present study was to investigate the microstructures, surface properties and hemocompatibility of the biomedical pure Ti substrates under different parameters of oxygen plasma modification.

2. Materials and Methods

2.1. Preparation of the Plasma-Oxidized Samples

The model PS350 plasma reactor system with 13.56 MHz radio frequency generator (AST, Boston, MA, USA) and the polished biomedical grade IV pure Ti disc substrates with a diameter of 14.5 mm and a thickness of 1 mm (Bio Tech One Inc., Kaohsiung, Taiwan) were used in this study. The Ti substrates were cleaned with acetone in an ultrasonic bath for 10 min followed by air drying before loading onto the sample holder in the vacuum chamber. Subsequently, the Ti substrates were cleaned in Ar plasma at a working time of 10 min, an argon flow rate of 30 sccm, chamber running pressure 5.0×10^{-3} torr and power 80 W to remove the native adsorbed contamination and produce a reproducible starting

condition for the subsequent oxidation procedure. After the cleaning process, the Ti substrates were immediately plasma-oxidized at six different power conditions (80, 120, 160, 200, 240 and 280 W) for three various periods (10, 20 and 30 min) under an oxygen flow rate of 30 sccm and the chamber running pressure 5.0×10^{-3} torr, respectively. Then, the plasma-oxidized samples were cooled in the reactor at room temperature for 10 min. A sample without plasma oxidation (i.e., the polished Ti disc) was also prepared as a control.

2.2. Surface Characterization Analysis of the Plasma-Oxidized Samples

The surface morphologies of the plasma-oxidized samples were observed using a field-emission scanning electron microscope (FE-SEM; JEOL JSM-6500F, JEOL Ltd. Tokyo, Japan). The compositions of the plasma-oxidized layers were analyzed by X-ray photoemission spectroscopy (XPS; MICROTOECH MT-500, VG Instruments Group Ltd, Manchester, UK) with a monochromatic Ag K α source. The XPS energy scale was calibrated by setting the binding energy of the Ag_{3d_{5/2}} line of clean silver to exactly 368.3 eV as referenced to the Femi level. The angle of incidence of the X-ray beam to the sample was 2°. High-resolution scans with a diameter of 15 nm X-ray beam were used for Ti and O elements detection.

2.3. Microstructure Identification of the Plasma-Oxidized Samples

Crystallinity analysis and phase identification were carried out by grazing incidence X-ray diffractometer (GIXRD; PHILIPS X'Pert Pro, Malvern Instruments Ltd., Almelo, The Netherlands) with CuK α 1 radiation operated at 50 kV and 250 mA and transmission electron microscope (TEM; JEM-2010F, JEOL Ltd. Tokyo, Japan) operated at 200 kV. All of the corresponding peaks were analyzed using the database from the Joint Committee on Powder Diffraction Standards. TEM samples were prepared by mechanical dimpling down to 20 μ m. Ar ion beam thinning (Gatan model 691, Gatan Inc., Pleasanton, CA, USA) was carefully controlled to produce electron-transparent areas.

2.4. Wettability Evaluation of the Plasma-Oxidized Samples

The sessile drop method using deionized water as a measurement substance was utilized for wettability examination. The droplet with a volume of ~ 5 μ L was dropped on each tested sample and the droplet was rested for 5 s (the droplet will become round by its own surface tension and eventually shapes into part of a sphere). Subsequently, the contact angle was measured in the profile of the droplet on the tested sample by means of the FTA-125 contact angle goniometer equipped with an optical subsystem (First Ten Angstroms Inc., Portsmouth, VA, USA). An average of five drops per sample was performed.

2.5. Hemocompatibility of the Plasma-Oxidized Samples

The variations of the red blood cells (RBCs) morphology at 20 min clotting time were observed to evaluate the hemocompatibility of the plasma-oxidized samples (each group of samples ($n = 3$)). The polished Ti disc substrate was used as the control sample. Before testing, the samples were first washed in an ultrasonic bath with acetone and then with ethanol for 15 min and air dried. Hereafter, all the samples were sterilized at room temperature for 24 h by using the G30T8 ultraviolet lamp (Atlantic Ultraviolet Corporation, Hauppauge, NY, USA) with a UV intensity of approximately 125 μ W/cm² at 1 m from the lamp. The sterilized samples were placed in 15 mL centrifuge tubes. Subsequently, 100 μ L blood was dropped onto the samples and clotted at room temperature for 20 min. The samples were then immersed in 10 mL deionized water at 37 °C for 10 min to dissolve the uncoagulated blood. Afterward, all the samples were fixed with 2% glutaraldehyde at room temperature for 1 h. Subsequently, the samples were washed and rinsed with PBS (phosphate-buffered saline) buffer solution thrice and air dried. Before being loaded into the chamber, the samples were sputter-coated with approximately 20–30-nm thick platinum thin films to provide electrical conductivity and prevent sample charging effects in FE-SEM.

3. Results and Discussion

Figure 1 shows superficial FE-SEM images of the control and plasma-oxidized samples. Apparently, the polished control sample revealed a smooth and flat surface feature (Figure 1a). After different plasma oxidation processes, a significant change in surface morphology was observed as shown in Figure 1b. The island-like topography feature was found on the sample that had been plasma-oxidized at 160 W for 30 min. Similar topography feature can also be observed on the plasma-oxidized samples under 160 W for various periods. As the plasma power increased above 200 W for various periods, it was discovered the presence of dimple-like topography feature on the surface layers of the plasma-oxidized samples (Figure 1c). The dimple-like topography became rougher at 280 W for 30 min.

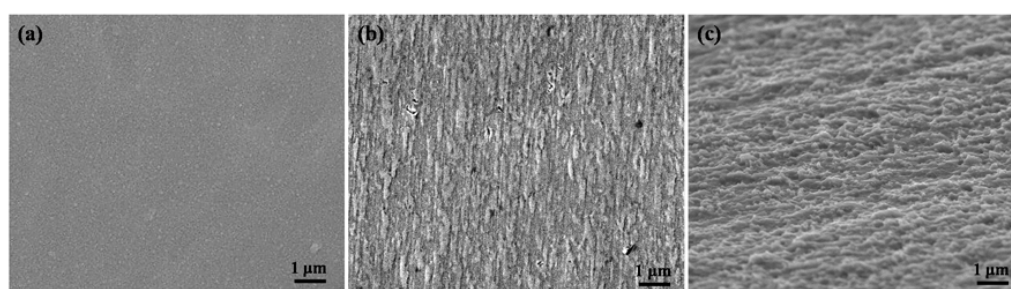


Figure 1. Superficial field-emission scanning electron microscope (FE-SEM) images of the control and plasma-oxidized samples: (a) the control sample (top-view); (b) the sample plasma-oxidized at 160 W for 30 min (top-view); and (c) the sample plasma-oxidized at 200 W for 30 min (side-view). The side-view image provides clearer surface morphology difference between the control sample and the plasma-oxidized sample.

Chemical bonding states of the plasma-oxidized samples were further analyzed using XPS. A computer assisted Gaussian-Lorentzian peak model was used to curve fit the spectrum. Figure 2a presents a typical high-resolution spectrum of Ti 2p from the plasma-oxidized sample at 80 W for 10 min. It revealed that different valence states of Ti^{2+} , Ti^{3+} and Ti^{4+} in the oxide layers could be detected by XPS. The Ti 2p peaks for Ti 2p_{1/2} and Ti 2p_{3/2} were observed at ~459 eV and ~465 eV, respectively. The binding energy indicated that the oxide layer on all plasma-oxidized samples mainly consisted of Ti^{4+} . When plasma treatment duration increased, the valence states of Ti^{2+} and Ti^{3+} decreased but Ti^{4+} increased as depicted in Figure 2b. On the other hand, a similar tendency of the valence states can also be found in those plasma-oxidized samples as increasing plasma treatment power (Figure 2c). Accordingly, the results revealed that the oxygen atoms existed on the plasma-oxidized Ti surface and its concentration increased with increasing plasma treatment power and duration.

Figure 3 shows the GIXRD pattern taken from the control sample and the samples that had been plasma-oxidized at different powers for 10 min. For the control sample, the typical α -Ti phase diffraction peaks of (100), (002) and (101) were detected. However, the α -Ti phase diffraction peaks of (100), (002) and (101) from the plasma-oxidized samples were shifted clearly (as indicated by arrows) as compared with the control Ti sample, which reveals the formation of rutile TiO_2 phase on the Ti surface layer. The same diffraction feature can also be obtained from those plasma-oxidized samples with longer processing time (20 min and 30 min). Based on the TEM analysis, the formation of a nanocrystalline structure by oxygen ion bombardment could be found in the sample that had been plasma-oxidized at 80 W for 10 min (Figure 4a). It indicates that in addition to the reflection spots of the α -Ti phase with hexagonal close-packed structure, the selected area electron diffraction pattern also consists of ring spots (as indicated by arrows) in the matrix. From the camera length and d -spacing between the ring spots, the nanocrystalline structure was confirmed to be a rutile TiO_2 phase with body-centered cubic structure. A similar feature can also be detected in the plasma-oxidized sample at 280 W for 30 min (Figure 4b). However, the ring spots in the selected area electron diffraction

pattern indicated only the presence of a nano-polycrystalline rutile TiO_2 phase in the surface layer. Hence, as the Ti sample underwent plasma oxidation at 280 W for 30 min, only the formation of a nanostructural rutile- TiO_2 oxide layer on the Ti surface.

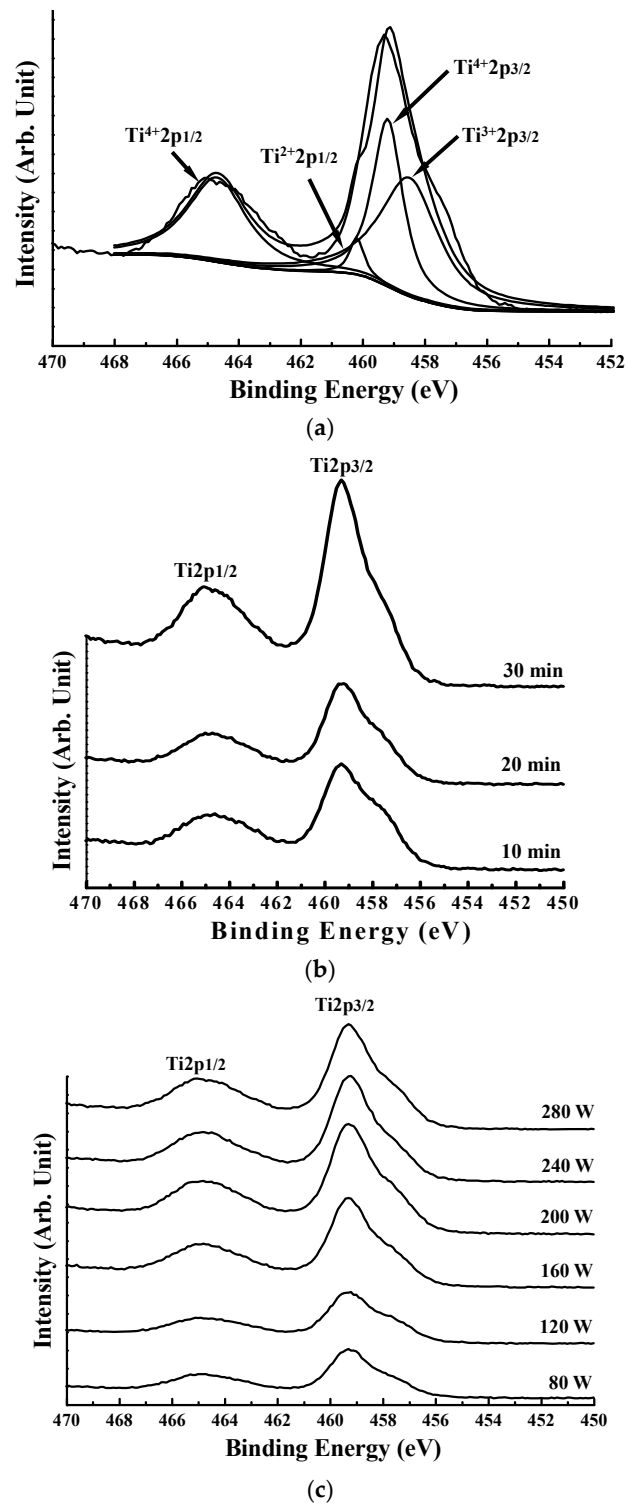


Figure 2. (a) Typical high-resolution X-ray photoemission spectroscopy (XPS) spectrum of Ti 2p from the plasma-oxidized sample at 80 W for 10 min, (b) XPS spectrum of Ti 2p from the plasma-oxidized sample at 80 W for various durations and (c) XPS spectrum of Ti 2p from the plasma-oxidized samples at different powers for 10 min.

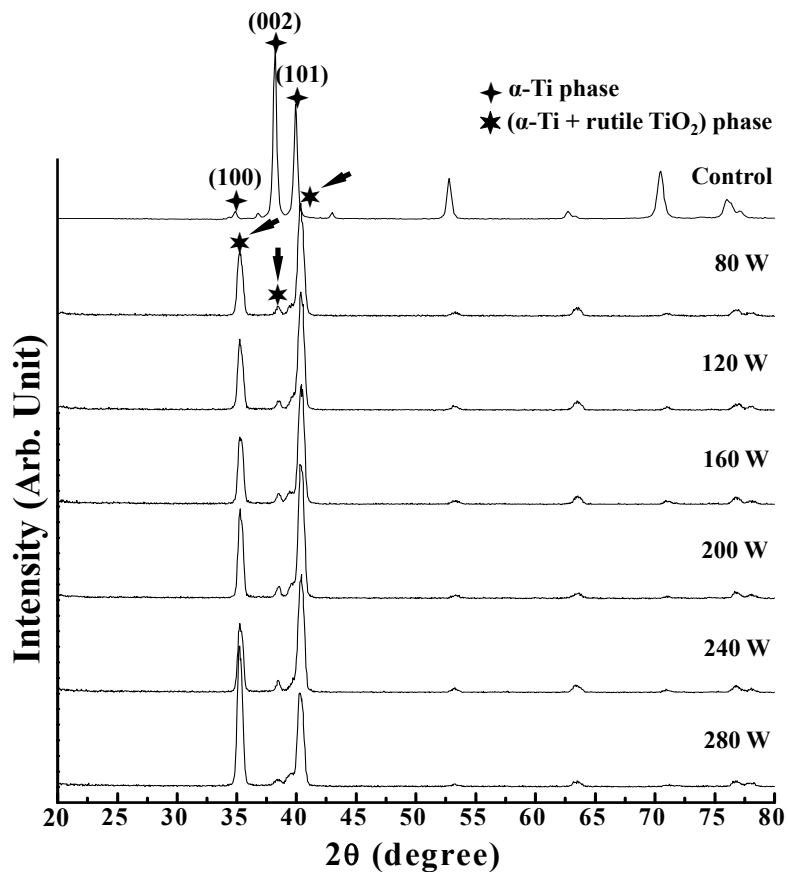


Figure 3. Grazing incidence X-ray diffractometer (GIXRD) pattern taken from the control sample and the samples that had been plasma-oxidized at different powers for 10 min. The peaks that indicated by arrows correspond to the (α -Ti + rutile TiO₂) phase.

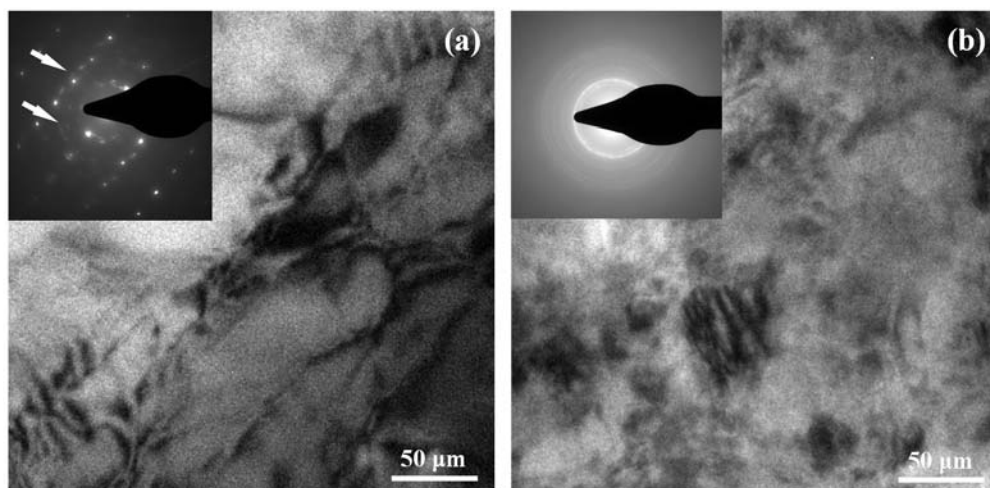


Figure 4. Transmission electron microscope (TEM) micrographs from the plasma-oxidized samples at (a) 80 W for 10 min and (b) 280 W for 30 min.

On the basis of the XPS, GIXRD and TEM results, there is a suggested mechanism for the formation of a TiO₂ layer on the Ti surface by oxygen plasma modification. When all the Ti atoms are oxidized, most of the oxygen reacts with the Ti material via diffusion and ion bombardment by plasma treatment [23,24]. At the same time, some of the oxygen species and/or radicals such as O₂, O*

and O^{2-} were produced by the plasma and then fixed at lattice or interstitial sites. This reaction is exothermic. It provides an important driving force for transporting oxygen species from the TiO_x/Ti interface towards the TiO_2/Ti one [18]. The effects increase the oxygen concentration ratio in the TiO_2 surface layer. Therefore, the oxygen plasma modification induces the oxygen easily reacts with Ti by diffusing into the Ti surface layer to form the TiO_2 layer.

Average contact angle measurements of the sample that had been plasma-oxidized at 280 W for various treatment times were shown in Figure 5. Evidently, it indicated that the samples possess surface hydrophilicity, since their angles are smaller than 90° [10,25]. The sample treated for 30 min exhibited a slightly higher hydrophilic surface than that of 10 min and 20 min treated samples, as well as the control Ti sample [16]. A similar feature can also be observed on the plasma-oxidized samples under 240 W for various periods. As compared with the topography feature of the oxide layers in Figure 1, this characteristic reveals that the sample with a rough dimple-like TiO_2 oxide layer induces a higher wettability formation. This could be attributed to the fact that materials with rough surfaces cause more gaps under the liquid drop, which could result in liquid easier flow into the gaps and formation of the hydrophilic interface. Moreover, the TiO_2 surface as a metal oxide surface is a high-energy one and thus should be fully wetted by most liquids [26]. The wettability responds to the surface bonding energy of Ti interface between the body fluid. The hydrophilic surface could enhance cell proliferation and tissue healing. Subsequently, it improved osseointegration of the interface between bone and implants [10,27]. Thus, the plasma-oxidized sample with a high hydrophilic surface could potentially promote its osseointegration in vivo.

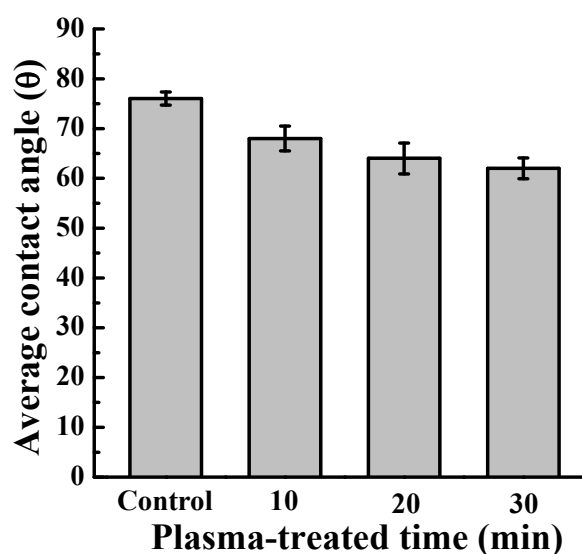


Figure 5. Wettability of the plasma-oxidized sample at 280 W for various treatment durations.

The FE-SEM images of RBCs morphology from the control and plasma-oxidized samples after blood contact for 10 min are shown in Figure 6. Clearly, the control sample (Figure 6a) induced fewer aggregations of RBCs at 10 min than that induced by the plasma-oxidized samples. The RBCs exhibited good adhesion on the sample that had been plasma-oxidized at 160 W for 30 min (Figure 6b). This characteristic could also be observed in the other treated samples. As the Ti sample plasma-oxidized at 280 W for 30 min, the RBCs not only attach on the sample surface but also have an excellently connected morphology with numerous platelets (as indicated by arrows) (Figure 6c). Thus, it is evident that hemocompatibility was investigated on the all of plasma-oxidized samples. The surface texture of the plasma-oxidized samples improved the aggregation of RBCs because of the increased surface hydrophilic property, which promotes the adsorption of RBCs and platelets. Moreover, rutile TiO_2 can improve the hemocompatibility of biomaterial surface,

subsequently enhanced the tissue healing [20]. The formation of Ti oxide was related to plasma treatment energy, ion bombardment and radical reactions. The results indicated that the transition of Ti structure can be formed by a higher energy plasma bombardment. It is widely believed that the osteoblasts prefer to interact with the surface-modified Ti oxide surface than Ti implant surface itself. The coagulation is the first step of bone healing. Ti oxide film on Ti affects the absorption rate of albumin/fibrinogen [16,28]. Park et al. have discussed the adhesion of blood cells such as platelets, red blood cells and leukocytes in terms of the surface topography of the implants [29,30]. The results indicate that the blood cells' adhesion increased on a rough surface of the Ti substrate in comparison to the Ti substrate with a smooth surface. Therefore, the oxygen plasma treatment has the potential to improve both biocompatibility and hemocompatibility of the Ti implant. Finally, more tests and studies must be carried out to study the wear resistance, mechanical strength and in vivo biocompatibility of the plasma-oxidized samples in the future.

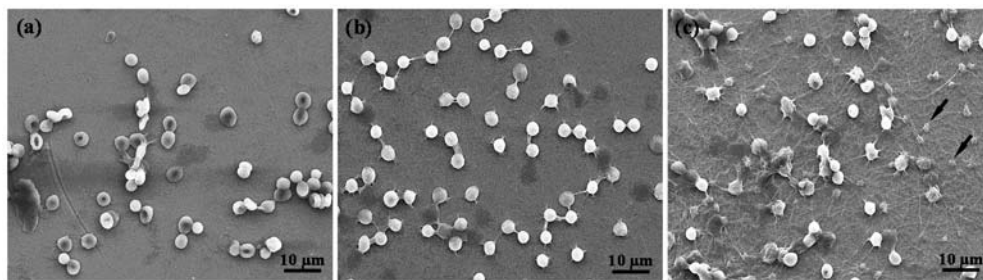


Figure 6. The FE-SEM images of red blood cells' (RBCs) morphology from the control sample and plasma-oxidized samples after blood contact for 20 min: (a) the control sample; (b) the sample plasma-oxidized at 160 W for 30 min; and (c) the sample plasma-oxidized at 280 W for 30 min.

4. Conclusions

A Ti oxide layer was formed on the pure Ti substrate by oxygen plasma modification. The topography of the oxide layer became rougher as increasing plasma treatment power and time. The microstructure analysis results showed the formation of nanostructural rutile TiO₂ phase on the surface of the Ti after different parameters of oxygen plasma treatment. It also exhibited that the rougher oxide layer on Ti surface resulted in a hydrophilic surface. The presence of a rough dimple-like oxide layer with nanostructural rutile TiO₂ phase has better hemocompatibility in the plasma-oxidized samples. It is believed that as the Ti implant with a nanostructural rutile TiO₂ layer could improve the tissue healing and then facilitate the osseointegration in vivo.

Author Contributions: Software, C.-M.L.; Validation, R.A.W.; Investigation, H.-J.C.; Data Curation, H.-H.C.; Writing-Original Draft Preparation, M.R. and C.-F.H.; Writing-Review & Editing, C.-M.L. and P.-W.P.; Supervision, K.-L.O. and E.S.

Funding: This research received no external funding.

Conflicts of Interest: The authors declare no conflict of interest.

References

1. Kammerer, P.W.; Schiegnitz, E.; Palarie, V.; Dau, M.; Frerich, B.; Al-Nawas, B. Influence of platelet-derived growth factor on osseous remodeling properties of a variable-thread tapered dental implant in vivo. *Clin. Oral Implant. Res.* **2017**, *28*, 201–206. [[CrossRef](#)] [[PubMed](#)]
2. Kim, S.E.; Yun, Y.P.; Lee, J.Y.; Shim, J.S.; Park, K.; Huh, J.B. Co-delivery of platelet-derived growth factor (PDGF-BB) and bone morphogenetic protein (BMP-2) coated onto heparinized titanium for improving osteoblast function and osteointegration. *J. Tissue Eng. Regen. Med.* **2015**, *9*, E219–E228. [[CrossRef](#)] [[PubMed](#)]

3. Al-Hezaimi, K.; Nevins, M.; Kim, S.W.; Fateh, A.; Kim, D.M. Efficacy of growth factor in promoting early osseointegration. *J. Oral Implantol.* **2014**, *40*, 543–548. [[CrossRef](#)] [[PubMed](#)]
4. Haimov, H.; Yosupov, N.; Pinchasov, G.; Juodzbaly, G. Bone Morphogenetic Protein Coating on Titanium Implant Surface: A Systematic Review. *J. Oral Maxillofac. Res.* **2017**, *8*, e1. [[CrossRef](#)] [[PubMed](#)]
5. Kim, S.Y.; Lee, Y.; Seo, S.J.; Lim, J.H.; Kim, Y.G. Effects of Escherichia Coli-derived Recombinant Human Bone Morphogenetic Protein-2 Loaded Porous Hydroxyapatite-based Ceramics on Calvarial Defect in Rabbits. *J. Bone Metab.* **2017**, *24*, 23–30. [[CrossRef](#)] [[PubMed](#)]
6. Biao, M.N.; Chen, Y.M.; Xiong, S.B.; Wu, B.Y.; Yang, B.C. Synergistic effects of fibronectin and bone morphogenetic protein on the bioactivity of titanium metal. *J. Biomed. Mater. Res.* **2017**, *105*, 2485–2498. [[CrossRef](#)] [[PubMed](#)]
7. Bafail, A.S.; Alamri, A.M.; Spivakovsky, S. Effect of antibiotics on implant failure and postoperative infection. *Evid. Based Dent.* **2014**, *15*, 58. [[CrossRef](#)] [[PubMed](#)]
8. Rimondini, L.; Fini, M.; Giardino, R. The microbial infection of biomaterials: A challenge for clinicians and researchers. A short review. *J. Appl. Biomater. Biomech.* **2005**, *3*, 1–10. [[PubMed](#)]
9. Huang, C.F.; Chiang, H.J.; Lan, W.C.; Chou, H.H.; Ou, K.L.; Yu, C.H. Development of silver-containing austenite antibacterial stainless steels for biomedical applications part I: Microstructure characteristics, mechanical properties and antibacterial mechanisms. *Biofouling* **2011**, *27*, 449–457. [[CrossRef](#)] [[PubMed](#)]
10. Lee, F.P.; Wang, D.J.; Chen, L.K.; Kung, C.M.; Wu, Y.C.; Ou, K.L.; Yu, C.H. Antibacterial nanostructured composite films for biomedical applications: Microstructural characteristics, biocompatibility, and antibacterial mechanisms. *Biofouling* **2013**, *29*, 295–305. [[CrossRef](#)] [[PubMed](#)]
11. Park, J.H.; Olivares-Navarrete, R.; Baier, R.E.; Meyer, A.E.; Tannenbaum, R.; Boyan, B.D.; Schwartz, Z. Effect of cleaning and sterilization on titanium implant surface properties and cellular response. *Acta Biomater.* **2012**, *8*, 1966–1975. [[CrossRef](#)] [[PubMed](#)]
12. Guthrie, K.I.; Sangha, N.; Genheimer, C.W.; Basu, J.; Ludlow, J.W. Migration assay to evaluate cellular interactions with biomaterials for tissue engineering/regenerative medicine applications. *Methods Mol. Biol.* **2013**, *1001*, 189–196. [[PubMed](#)]
13. Echeverry-Rendon, M.; Galvis, O.; Aguirre, R.; Robledo, S.; Castano, J.G.; Echeverria, F. Modification of titanium alloys surface properties by plasma electrolytic oxidation (PEO) and influence on biological response. *J. Mater. Sci. Mater. Med.* **2017**, *28*, 169. [[CrossRef](#)] [[PubMed](#)]
14. Hou, P.J.; Ou, K.L.; Wang, C.C.; Huang, C.F.; Ruslin, M.; Sugiatno, E.; Yang, T.S.; Chou, H.H. Hybrid micro/nanostructural surface offering improved stress distribution and enhanced osseointegration properties of the biomedical titanium implant. *J. Mech. Behav. Biomed. Mater.* **2017**, *79*, 173–180. [[CrossRef](#)] [[PubMed](#)]
15. Dong, X.; Guojiang, W.; Maitz, M.F.; Yifeng, L.; Nan, H.; Hong, S. Characterization and mechanical investigation of Ti-O_{2-x} film prepared by plasma immersion ion implantation and deposition for cardiovascular stents surface modification. *Beam Interact. Mater. Atoms* **2012**, *289*, 91–96.
16. Tsai, M.H.; Haung, C.F.; Shyu, S.S.; Chou, Y.R.; Lin, M.H.; Peng, P.W.; Ou, K.L.; Yu, C.H. Surface modification induced phase transformation and structure variation on the rapidly solidified recast layer of titanium. *Mater. Charact.* **2015**, *106*, 463–469. [[CrossRef](#)]
17. Lu, T.; Qiao, Y.; Liu, X. Surface modification of biomaterials using plasma immersion ion implantation and deposition. *Interface Focus* **2012**, *2*, 325–336. [[CrossRef](#)] [[PubMed](#)]
18. Gottlicher, M.; Rohnke, M.; Kunz, A.; Thomas, J.; Henning, R.A.; Leichtweiss, T.; Gemming, T.; Janek, J. Anodization of titanium in radio frequency oxygen discharge—Microstructure, kinetics & transport mechanism. *Solid State Ion.* **2016**, *290*, 130–139.
19. Hung, W.C.; Chang, F.M.; Yang, T.S.; Ou, K.L.; Lin, C.T.; Peng, P.W. Oxygen-implanted induced formation of oxide layer enhances blood compatibility on titanium for biomedical applications. *Mater. Sci. Eng. C Mater. Biol. Appl.* **2016**, *68*, 523–529. [[CrossRef](#)] [[PubMed](#)]
20. Maitz, M.F.; Pham, M.T.; Wieser, E.; Tsyganov, I. Blood compatibility of titanium oxides with various crystal structure and element doping. *J. Biomater. Appl.* **2003**, *17*, 303–319. [[CrossRef](#)] [[PubMed](#)]
21. Roy, S.C.; Paulose, M.; Grimes, C.A. The effect of TiO₂ nanotubes in the enhancement of blood clotting for the control of hemorrhage. *Biomaterials* **2007**, *28*, 4667–4672. [[CrossRef](#)] [[PubMed](#)]

22. Eriksson, C.; Lausmaa, J.; Nygren, H. Interactions between human whole blood and modified TiO₂-surfaces: Influence of surface topography and oxide thickness on leukocyte adhesion and activation. *Biomaterials* **2001**, *22*, 1987–1996. [[CrossRef](#)]
23. Baier, R.E.; Carter, J.M.; Sorensen, S.E.; Meyer, A.E.; McGowan, B.D.; Kasprzak, S.A. Radiofrequency gas plasma (glow discharge) disinfection of dental operative instruments, including handpieces. *J. Oral Implantol.* **1992**, *18*, 236–242. [[PubMed](#)]
24. Ou, K.L.; Shih, Y.H.; Huang, C.F.; Chen, C.C.; Liu, C.M. Preparation of bioactive amorphous-like titanium oxide layer on titanium by plasma oxidation treatment. *Appl. Surf. Sci.* **2008**, *255*, 2046–2051. [[CrossRef](#)]
25. Shen, J.W.; Chen, Y.; Yang, G.L.; Wang, X.X.; He, F.M.; Wang, H.M. Effects of storage medium and UV photofunctionalization on time-related changes of titanium surface characteristics and biocompatibility. *J. Biomed. Mater. Res. B* **2016**, *104*, 932–940. [[CrossRef](#)] [[PubMed](#)]
26. Stevens, N.; Priest, C.I.; Sedev, R.; Ralston, J. Wettability of photoresponsive titanium dioxide surfaces. *Langmuir* **2003**, *19*, 3272–3275. [[CrossRef](#)]
27. Ou, S.F.; Chou, H.H.; Lin, C.S.; Shih, C.J.; Wang, K.K.; Pan, Y.N. Effects of anodic oxidation and hydrothermal treatment on surface characteristics and biocompatibility of Ti-30Nb-1Fe-1Hf alloy. *Appl. Surf. Sci.* **2012**, *258*, 6190–6198. [[CrossRef](#)]
28. Wu, W.F.; Ou, K.L.; Chou, C.P.; Wu, C.C. Effects of nitrogen plasma treatment on tantalum diffusion barriers in copper metallization. *J. Electrochem. Soc.* **2003**, *150*, G83–G89. [[CrossRef](#)]
29. Park, J.Y.; Davies, J.E. Red blood cell and platelet interactions with titanium implant surfaces. *Clin. Oral Implant. Res.* **2000**, *11*, 530–539. [[CrossRef](#)]
30. Park, J.Y.; Gemmell, C.H.; Davies, J.E. Platelet interactions with titanium: Modulation of platelet activity by surface topography. *Biomaterials* **2001**, *22*, 2671–2682. [[CrossRef](#)]



© 2018 by the authors. Licensee MDPI, Basel, Switzerland. This article is an open access article distributed under the terms and conditions of the Creative Commons Attribution (CC BY) license (<http://creativecommons.org/licenses/by/4.0/>).